The 2009 IEEE/RSJ International Conference on
Intelligent Robots and Systems
October 11-15, 2009 St. Louis, USA

Improving Machining Accuracy with Robot Deformation Compensation

Jianjun Wang, Hui Zhang, and Thomas Fuhlbrigge, *Member, IEEE*

***Abstract*—Industrial robots offer a cheaper yet more flexible alternative to the CNC machines in the cleaning and pre-machining applications of automotive aluminum castings. But the low stiffness has limited the application of industrial robots to the machining tasks with very low precision requirement. This paper presents a practical method to compensate the robot deformation caused by the machining force. A constant joint stiffness model based feed forward compensation scheme is implemented in the robot controller. The compensation scheme is shown to be able to reduce the position error by more than 60%. Application test in milling a standard aluminum block has demonstrated the effectiveness of the proposed deformation compensation method. The surface error is reduced from 0.5mm to 0.1mm.**

I. Introduction

The automotive industry represents the fastest-growing market segment of the aluminum industry, due to the increasing usage of aluminum in cars for lower fuel consumption and better vehicle performance. Most of the automotive aluminum parts start from a casting in a foundry plant, followed by the downstream processes usually including cleaning and pre-machining of the gating system and riser. Robot based flexible automation offers an ideal solution for the cleaning and pre-machining applications due to its programmability, adaptability, flexibility and relatively low cost. Nevertheless, the foundry industry has not seen many success stories for such applications and installations.

The major hurdle preventing the adoption of robots for the machining processes is the fact that the stiffness of today's industrial robot is much lower than that of a standard CNC machine. Field tests using industrial robots for heavy machining such as milling often found that a perfect robot program without considering contact and deformation fails to produce the desired path once the robot starts to execute the machining task. Due to the much lower stiffness, a 500N cutting force during a milling process will cause a 1 mm position error for a robot compared to a less than 0.01mm error for a CNC machine. Since the robot typically has 0.1mm motion error without contact, the majority of the position error in heavy machining operations comes from the contact force induced deformation. Therefore, to achieve higher accuracy in robotic machining, the deformation must be accurately compensated.

The existing research of robot deformation compensation is mostly focused on gravity and deflection compensation of flexible manipulators [1], [2]. To increase the position accuracy, rigid manipulators are treated flexible so that the compliance from the joints and links are included in the compensation model [3]. In these research efforts, the external load applied on the manipulator is basically a dead weight fixed to the robot end effector. Not much attention has been paid to the compensation of process force induced robot deformation.

Methods for compensating the robot deformation can be classified as model based and sensor based. Model based compensation uses a model to predict the robot deformation and then modify the robot position reference accordingly. [4]-[7] described the modeling and identification of the robot stiffness for milling and cutting applications. A complex joint stiffness model was used to include not only the elasticity in the direction of the joint motion but also the compliances orthogonal to the joint motion.

Unlike the model based method, the sensor based methods measure the deformation induced position error in either the joint space or the Cartesian space and then adjust the position reference accordingly. In [8], a linear scale unit was placed on each prismatic link of a hexapod parallel kinematics machine to measure the link deformation caused by external forces and heat. It is natural to apply the feedback scheme for the sensor based methods to continuously adjust the robot position until the position error is within the specified limit. However, the setting time will be a concern if the robot is moving with high speed.

Although sensor based compensation methods offer higher position accuracy, they are very difficult to implement on an existing robot manipulator. Even it is possible to install the sensor, the final system cost would be expensive because of the sensor cost. This makes the sensor based methods more suitable for high accuracy discrete processes such as drilling, while the model based methods are better for continuous processes such as milling and roller hemming.

The goal of this paper is to present a practical method to improve the machining accuracy through robot deformation compensation. This paper does not strive to achieve the maximal possible deformation compensation, but rather a reasonable cost to benefit ratio as often requested in an industrial product. Under this guideline, a constant diagonal

Manuscript received March 1, 2009. This work was supported by ABB Corporate Research Funding.

All authors are with Corporate Research Center of ABB Inc., Windsor, CT 06095. All corresponds should be addressed to Jianjun Wang. (phone: 860-285-6964; fax: 860-285-6939; e-mail: Jianjun.Wang@ us.abb.com).

joint stiffness model is used for easy identification and real time implementation in the industrial robot controller.

The remaining paper is organized as following. Section 2 and 3 describe the modeling and identification of the robot deformation, while section 4 is devoted to the implementation of deformation compensation in the robot controller. The performance of the model based deformation compensation is verified through a simplified milling test in section 5.

II. ROBOT DEFORMATION MODELING

A robot manipulator deforms under external forces because of its compliance. The sources of the compliance are the compliances at the manipulator base, gearboxes, motors, links and other transmission elements, in addition to the active stiffness provided by the position control loop. For many industrial manipulators it is reasonable to assume that: 1) the compliance in the joints (gearbox and motor) is the dominant source of the robot deformation, 2) the links are infinitely stiff, 3) a joint PID control loop is used and the active joint stiffness provided by the control loop has small variation over time at the steady state. These assumptions are similar to those stated in [9]. It is worthwhile to point out that, robot manufacturers are moving toward the new generation slim manipulators and these 3 assumptions might be invalid. Especially, the links might contribute equally to the deformation as the joints.

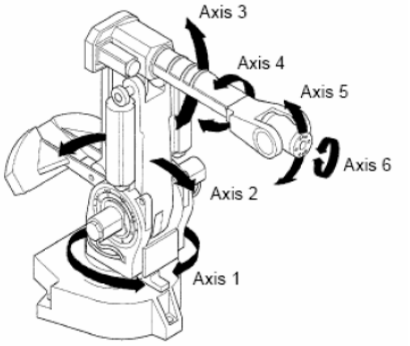

Fig. 1. A 6-axis serial robot manipulator.

A. Joint Stiffness

With the above three assumptions, the stiffness of a 6-axis serial robot manipulator shown in Fig. 1 can be represented by its link side joint stiffness: a constant 6*6 diagonal matrix with each diagonal term defining the stiffness of a joint.

$$K_\theta = Diag\left(\begin{bmatrix} k_{\theta 1} & k_{\theta 2} & k_{\theta 3} & k_{\theta 4} & k_{\theta 5} & k_{\theta 6} \end{bmatrix}^T\right) \quad (1)$$

B. Cartesian Stiffness

As the deformation is often observed and compensated at the tool tip, the Cartesian stiffness at the tooltip K_t is important. It can be computed as

$$K_t = J_t^{-T} K_\theta J_t^{-1} \quad (2)$$

where J_t is the Jacobian matrix that transforms a small joint angle displacement $\Delta\boldsymbol{\theta}$ to the translational and rotational displacements $\Delta\mathbf{x}_t$ of a Cartesian frame attached to the tool tip

$$\Delta\mathbf{x}_t = J_t \Delta\boldsymbol{\theta} \quad (3)$$

The deflection caused by the external force vector can be calculated through the Cartesian stiffness as:

$$\mathbf{F}_t = K_t \Delta\mathbf{x}_t = J_t^{-T} K_\theta J_t^{-1} \Delta\mathbf{x}_t \quad (4)$$

The joint stiffness matrix K_θ reflects the natural entity of a manipulator structure. It is diagonal, positive definite and constant irrespective of the external force or the robot configuration. In contrast, the Cartesian stiffness matrix K_t is configuration dependent.

Note that here we did not use the enhanced stiffness modeling as shown in [9][10], where an external force and robot configuration dependent stiffness term is included in the Cartesian stiffness formulation. This is because under the rated robot payload range, the contribution of this extra stiffness term to the total robot deformation is very small. In addition, the conventional formulation (2) has the computational advantage.

C. Deformation Characteristics of a serial manipulator

Unlike the Cartesian robots, serial manipulators demonstrate counter intuitive deformation phenomena at certain configurations and load conditions due to the coupling of its joints during a Cartesian motion. Fig. 2 simulates the deformation of an ABB IRB 4400-195-60 robot under a series of load conditions. The robot joint stiffness matrix is assumed as:

$$K_\theta = [386.83 \quad 614.62 \quad 372.29 \quad 112.56 \quad 97.79 \quad 24.77] \times 10^3 \ \text{N} \cdot \text{m/rad}$$

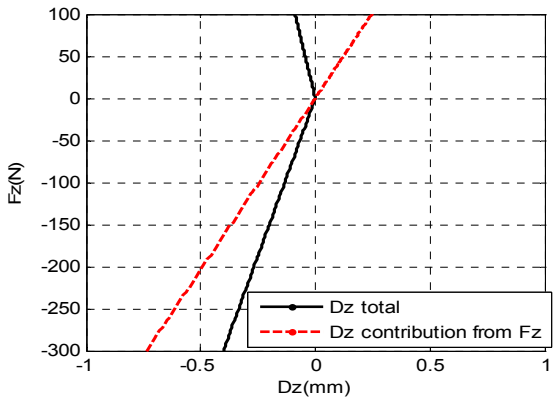

Fig. 2. Simulated load-deformation curve for an IRB 4400 demonstrates the apparent negative and piecewise linear stiffness in a Cartesian direction. The loading starts from (-100N,200N,-300N), then ramps down to (0,0,0) and finally ramps up to (100N,-200N,100N). The counter intuitive phenomenon is due to the off-diagonal terms in the Cartesian stiffness matrix mathematically, and the coupling of the robot joint motion physically. The contribution of Fx and Fy forces to the deformation in z direction (Dz) is significant.

Figure 2 clearly shows that in a Cartesian direction a serial manipulator can exhibit 1) the *apparent* negative stiffness and 2) totally different stiffness for different

loading curves. These unique deformation characteristics are the key to the explanation of many seemingly strange phenomena occurred during contact operations performed by a serial manipulator.

III. ROBOT DEFORMATION IDENTIFICATION

A. Mathematical Formulation

A least square solution of (4) can be used to identify the joint stiffness provided that the full force/torque vector and the full translation and rotation displacement can be measured in the same coordinate frame. In reality, this is hard to achieve since the measurement of a rotational deformation is difficult. In addition, the torque measurement is often less accurate than the force measurement. Due to the space constraint, the setup of the stiffness identification often requires the external force acting on a location different from the deformation measurement location. As a result, (4) has to be modified to account for these constraints.

For convenience, we define two tool frames: the force action frame T_f as identified by subscript f and the deformation measurement frame T_m as identified by subscript m. The external load and the corresponding deformation can be then expressed in T_f and T_m respectively as

$$\mathbf{F}_f = \begin{bmatrix} F_x \\ F_y \\ F_z \\ T_x \\ T_y \\ T_z \end{bmatrix}_f \qquad \mathbf{D}_m = \begin{bmatrix} D_x \\ D_y \\ D_z \\ \Delta\phi_x \\ \Delta\phi_y \\ \Delta\phi_z \end{bmatrix}_m \tag{5}$$

Using the duality between the joint space and the Cartesian space, the joint torque needed to balance the external force $\mathbf{F}_f$ is calculated as

$$\boldsymbol{\Gamma} = J_f^T \mathbf{F}_f \tag{6}$$

The joint deformation caused by this joint torque is obtained through joint stiffness matrix as

$$\Delta\boldsymbol{\theta} = K_\theta^{-1}\boldsymbol{\Gamma} \tag{7}$$

This joint deformation will be reflected at the measurement frame and the corresponding Cartesian deflection can be calculated through the Jacobian matrix as

$$\mathbf{D}_m = J_m \Delta\boldsymbol{\theta} = J_m K_\theta^{-1}\boldsymbol{\Gamma} = J_m K_\theta^{-1} J_f^T \mathbf{F}_f \tag{8}$$

If only the translational displacement can be measured, then (8) should be changed to

$$\begin{aligned} \Delta\mathbf{X}_m &= \begin{bmatrix} D_x & D_y & D_z \end{bmatrix}_m^T = \begin{bmatrix} I_{3\times3} & 0_{3\times3} \end{bmatrix} J_m K_\theta^{-1} J_f^T \mathbf{F}_f \\ &= \begin{bmatrix} I_{3\times3} & 0_{3\times3} \end{bmatrix} J_m diag\left\{ J_f^T \mathbf{F}_f \right\} \mathbf{C}_\theta \end{aligned} \tag{9}$$

where $\mathbf{C}_\theta = \begin{bmatrix} 1/k_{\theta1} & 1/k_{\theta2} & 1/k_{\theta3} & 1/k_{\theta4} & 1/k_{\theta5} & 1/k_{\theta6} \end{bmatrix}^T$ is the joint compliance vector. The diagonality of the stiffness matrix is used in the derivation of (9).

If the measurement is taken N times, the least square solution of the joint compliance vector is

$$\mathbf{C}_\theta = \left(\sum_{i=1}^{N} A_i^T A_i \right)^{-1} \left(\sum_{i=1}^{N} A_i^T b_i \right) \tag{10}$$

The fitting error is given by

$$e = \sum_{i=1}^{N} e_i^T e_i = \sum_{i=1}^{N} b_i^T b_i - \left(\sum_{i=1}^{N} A_i^T b_i \right)^T \left(\sum_{i=1}^{N} A_i^T A_i \right)^{-1} \left(\sum_{i=1}^{N} A_i^T b_i \right) \tag{11}$$

where

$$\begin{aligned} A_i &= \begin{bmatrix} I_{3\times3} & 0_{3\times3} \end{bmatrix} J_m(\boldsymbol{\theta}_i) diag\left\{ J_f^T(\boldsymbol{\theta}_i) \mathbf{F}_f{}^i \right\} \\ b_i &= \Delta\mathbf{X}_m{}^i \end{aligned} \tag{12}$$

B. Experimental setup for stiffness measurement

Fig. 3 shows a setup for identifying the stiffness of an ABB IRB4400 robot. An ATI Omega force sensor is mounted on the robot wrist and used to measure the external force acting on the robot. To measure the deformation, a portable coordinate measurement arm from Romer, the CimCore series 3000i, is attached to the robot end effecter. The claimed accuracy of this digitizer is about ±0.016mm in a measurement volume of 0.9 m^3. The external force is exerted by an air cylinder through a pulley relayed string. The magnitude of the external force can be adjusted by changing the air pressure, while the direction of the force can be altered by the position of the pulley on the column. In this setup there will no torque applied at the force action point due to the use of the string and the point connection of the string to the robot end effector. Using the static

Fig. 3. Experimental setup for robot stiffness identification. The force action frame T_f is parallel to the deformation measurement frame T_m but with a different origin.

equilibrium, the force vector at the force action frame is the same as the one at the force sensor frame. This setup is intentionally designed to avoid the usage of the torque measurement since the torque component measurement in

ATI force sensor has much poorer accuracy than the force component measurement.

Before the test, the setup needs to be calibrated. This includes the calibration of the digitizer base frame relative to the robot base, the pose of the force action frame and the pose of the measurement frame.

Although the joint stiffness matrix can be identified at a single robot configuration by altering the load magnitude and direction, performing the test at multiple configurations allow the verification of the assumptions made for the deformation model, and the reduction of identification error through averaging. At each robot configuration, in order to have a full picture of the deformation, the application of the external load forms a full cycle of loading and unloading as shown in Fig. 4a. At each load condition, a one minute waiting time is imposed for the stabilization of the load and the deformation. The measurement from the force sensor and the digitizer are then taken 6 times to average the measurement noise. Since the digitizer measurement is actually the robot position, the deformation of the robot for a given load can be obtained by simply subtracting the robot position measurement at the initial unloaded condition.

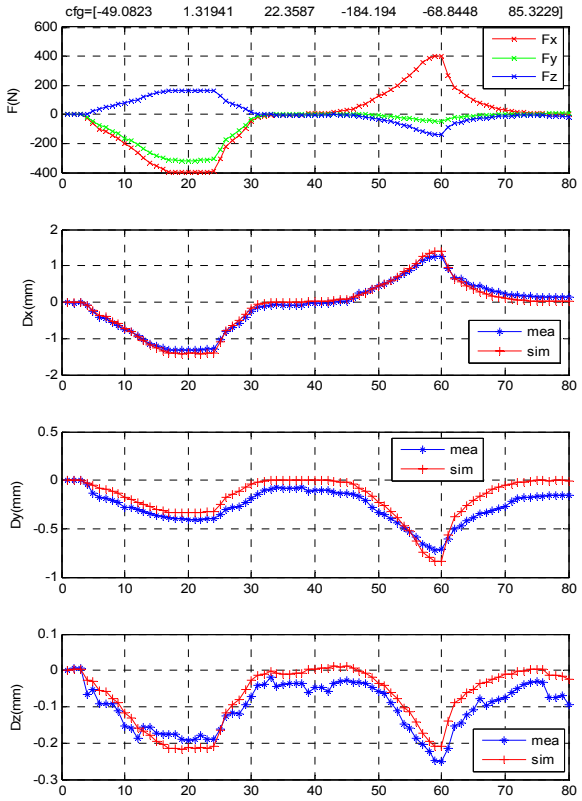

Fig. 4a. Loading and deformation curves at test configuration 1. Note that the force action frame is parallel to the deformation measurement frame but with an offset.

C. *Stiffness Identification Result*

The stiffness identification is performed at 6 different joint configurations. Fig. 4 shows the loading curve, deformation curve, and the load vs. deformation curve for the first test configuration.

The linear least square fitting is performed on the entire 6 test sets to find the solution of the joint stiffness as:

$$K_\theta = [731.82 \quad 488.31 \quad 428.61 \quad 59.52 \quad 56.87 \quad 16.55] \times 10^3 \ \text{N} \cdot \text{m/rad}$$

For comparison, Fig. 4 also shows the model predicted deformation based on the identified joint stiffness. It can be seen that the modeling error is within ±0.2mm over the ±1.5mm deformation range. Therefore, the deformation compensation can be expected to reduce the deformation error by more than 60%.

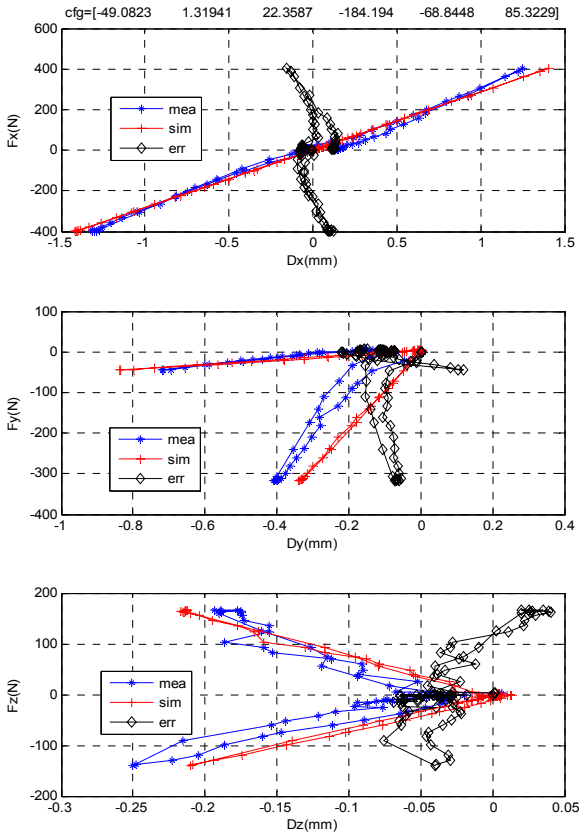

Fig. 4b. Loading vs deformation curves at test configuration 1. Note that the force action frame is parallel to the deformation measurement frame but with an offset.

IV. DEFORMATION COMPENSATION

The constant and diagonal joint stiffness model lends itself to the real time implementation due to the low computation cost. The block diagram of the real time deformation compensation is shown in Fig. 5. After filtering the force sensor noise and compensating the gravity of the force sensor payload, the force signal was translated into the robot tool frame. Based on the stiffness model identified before, the deformation due to the external contact force is calculated in real time and the joint reference for the robot controller is updated. Fig. 5 has been implemented in the ABB's IRC5 robot controller using the existing force control platform. The deformation is calculated every 4ms.

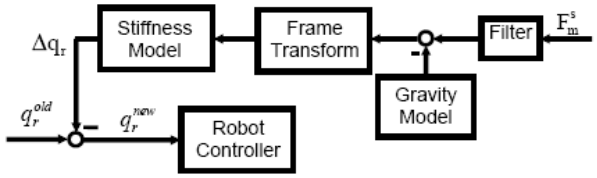

Fig. 5. Block diagram of a real time deformation compensation.

A. Static performance of deformation compensation

To verify the performance of the deformation compensation, the same test setup for the identification is used. The difference is that at each joint configuration the test procedure is performed twice, one without the compensation and one with the compensation activated. Fig. 6 compares the measured deformation before and after the compensation at one joint configuration. The magnitude of the deformation is shown to be reduced from 1.8mm to 0.4mm at the maximal load condition. The compensation actually changed the direction of the deformation vector.

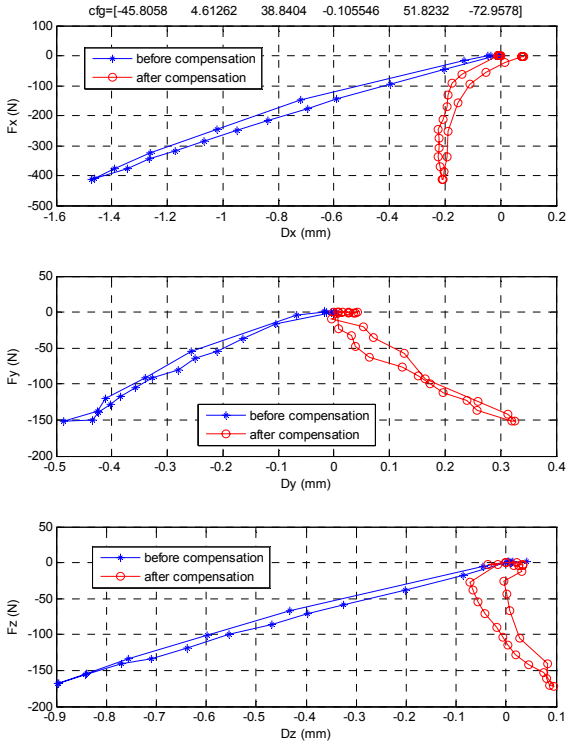

Fig. 6. Measured load-deformation curve before and after compensation at configuration [-45.8058, 4.61262, 38.8404, -0.105546, 51.8232, -72.9578].

B. Dynamic performance of deformation compensation

Since the deformation compensation is implemented in the 4ms loop, fast response can be expected. This can be verified by applying the robot with an impulse load. The impulse load can be realized by the sudden drop of a dead weight. This is achieved by replacing the air cylinder with a dead weight in Fig. 3. This approach makes sure all the calibrations are not affected. Fig. 7 shows the deformation response under such an impulse load. The compensation delay is about 50ms, which is significantly greater than 4ms. Part of the delay comes from the poor synchronization between the force sensor measurement and the digitizer measurement. The measurement from the force sensor is directly sampled by the robot controller with 4ms rate. But the digitizer measurement is first acquired by a PC using a serial port and then forwarded to the robot controller through a fast Ethernet connection. Efforts are needed to measure the exact delay caused by this poor synchronization so that its significance can be evaluated.

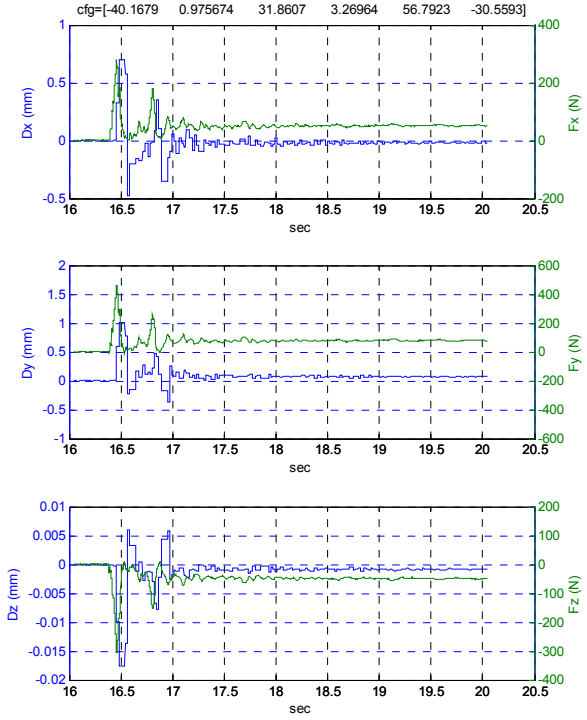

Fig. 7. Dynamic deformation response under an impulse load at joint configuration [-40.1679, 0.9757, 31.8607, 3.2696, 56.7923, -30.5593].

V. Application Test

Fig. 8 shows the setup of a milling test where a 6063 aluminum block is used for testing purpose. A laser displacement sensor is used to measure the finished surface. The surface error without deformation compensation demonstrates the counter intuitive "negative stiffness phenomenon"; an extra 0.5mm was removed in the middle of the milling path. This can be easily explained by the off-diagonal terms of the Cartesian stiffness matrix resulting from the coupling of the robot joint motion. Although the normal contact force F_n pushed the cutter away from the surface, the force in the feed direction F_f and the cutting direction F_c actually caused the robot to deform into the part surface. Since the feed force and the cutting force are significant in this setup compared to the normal force, the overall effect is that the actual depth of cut is 0.5mm more than the commanded. Fig. 9 compares the surface error with

and without the deformation compensation. A less than 0.1 mm surface error is achieved with the deformation compensation. This error is in the range of robot path accuracy. The negative surface error in the figure means less material was removed than the commanded one.

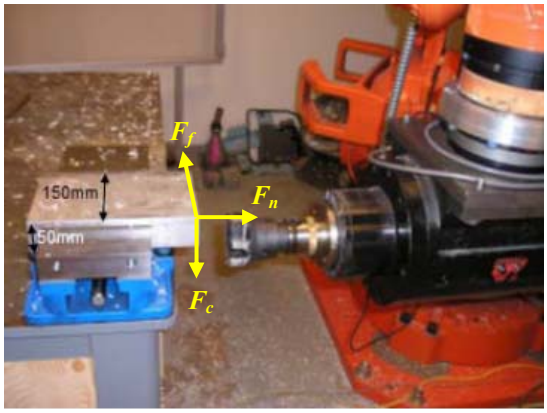

Fig. 8. A milling test on a 6063 aluminum block to verify the effectiveness of the deformation compensation.

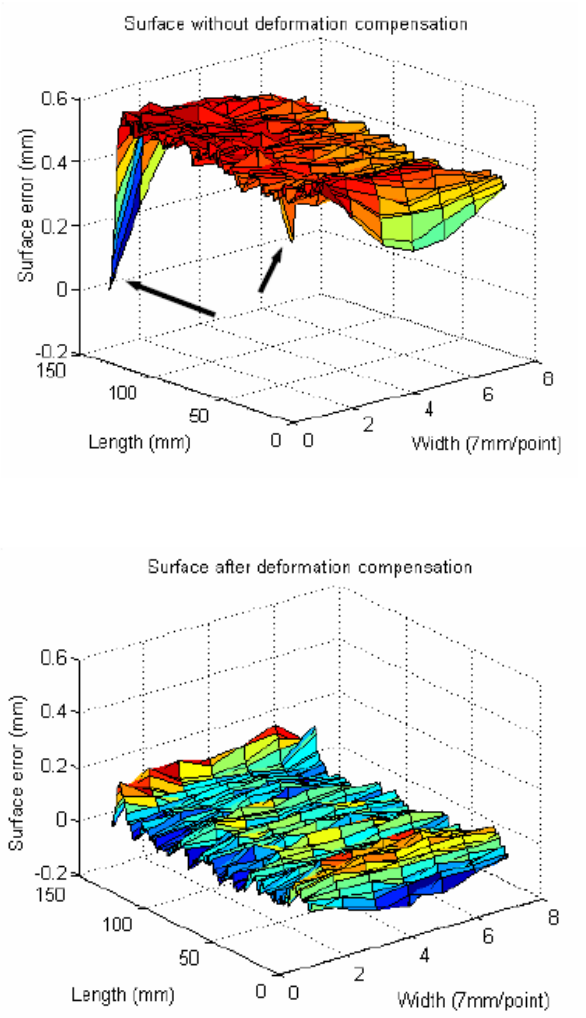

Fig. 9. Surface error before and after deformation compensation in a milling test.

VI. Conclusion and Discussion

This paper describes in detail the modeling, identification and compensation of robot deformation caused by the external process forces from the machining applications. Lab measurement and application tests have shown that, with a simple joint stiffness model based feed forward approach the deformation compensation can reduce the contact force induced position error by more than 60%. While robot deformation compensation is technically feasible, more efforts are needed to make it available as a product to be used in the field. The main challenge is to simplify the stiffness identification process. The recommendation for future work is to investigate the existing compliance models in the robot controller [3] and try to implement the deformation compensation using these models.

References

[1] D. Surdilovic and M. Vukobratovic, "Deflection compensation for large flexible manipulators," *Mechanism and Machine Theory*, vol. 31, no. 3, pp. 317-329, 1996.

[2] J. C. Hwang, J. H Seo, Y. W. Choi, and H. J. Yim, "Error compensation of a large scale LCD glass transfer robot," in *Proc. 17th World Congress, The International Federation of Automatic Control*, Seoul, Korea, July 2008, pp. 6749-6750.

[3] M. Abderrahim, A. Khamis, S. Garrido and L. Moreno, "Accuracy and calibration issues of industrial manipulators," in *Industrial Robotics: Programming, Simulation and Applications*, L. K. Huat, Ed. Germany: Pro Literatur Verlag, 2007, pp. 131-146.

[4] E. Abele, M. Weigold, and M. Kulok, "Increasing the accuracy of a milling industrial robot," *Production Engineering*, vol. 13, no. 2, pp. 221-224, 2006.

[5] M. Stelzer, O. von Stryk, E. Abele , J. Bauer, and M. Weigold, "High speed cutting with industrial robots: towards model based compensation of deviations," in *Proceedings of Robotik*, Munich, Germany, 2008, pp. 143-146.

[6] E. Abele, M. Weigold and S. Rothenbücher, "Modeling and identification of an industrial robot for machining applications," *CIRP Annals - Manufacturing Technology*, vol. 56, no. 1, pp. 387-390, 2007.

[7] E. Abele, S. Rothenbücher, and M. Weigold, "Cartesian compliance model for industrial robots using virtual Joints," *Production Engineering*, vol. 2, no. 3, pp. 339-343, 2008.

[8] T. Oiwa, "Error compensation system for joints, links and machine frame of parallel kinematics machines," *Int. J. Robotics Research*, vol. 24, no. 12, pp. 1087-1102, 2005.

[9] G. Alici and B. Shirinzadeh, "Enhanced stiffness modeling, identification and characterization for robot manipulators," *IEEE Trans. Robotics*, vol. 21, no. 4, pp. 554-564, Aug. 2005.

[10] S.F. Chen, "The 6x6 stiffness Formulation and Transformation of Serial Manipulators via the CCT Theory," *Proc. of the 2003 IEEE Int. Conf. on Robotics & Automation*, Taipei, Taiwan, Sept. 2003, pp. 4042-4047